# Discussion about the magnetic field produced by cylindrical halbach structures

Romain Ravaud, Guy Lemarquand

*Progress In Electromagnetics Research B, Vol. 13, 275–308, 2009*

# DISCUSSION ABOUT THE MAGNETIC FIELD PRODUCED BY CYLINDRICAL HALBACH STRUCTURES

**R. Ravaud and G. Lemarquand**

Laboratoire d'Acoustique de l'Universite du Maine, UMR CNRS 6613
Avenue Olivier Messiaen, 72085 Le Mans, France

**Abstract**—This paper uses a three-dimensional analytical approach based on the Coulombian model for studying the magnetic field produced by cylindrical Halbach structures. Such structures, commonly used in magnetic couplings or in electrical machines, are composed of tile permanent magnets with rotating magnetizations. Such assemblies of tile permanent magnets allow one to easily optimize the radial field shape in the air gap of electrical machines. In addition, Halbach structures can be used in magnetic couplings for improving the torque transmitted between the two rotors. Analytical studies dealing with the optimization of such structures generally use a two-dimensional analytical approach for calculating either the magnetic field produced by tile permanent magnets or the forces exerted between them. These two-dimensional expressions are useful because they have a very low computational cost. However, their accuracy depends greatly on the structure dimensions. We propose in this paper to use a three-dimensional analytical model based on the Coulombian model for determining the exact shape of the magnetic field produced by a Halbach structure. Such an approach also allows one to determine the demagnetizing magnetic field inside the tile permanent magnets. This element of information is important for the design of tile permanent magnets. In addition, we show that some effects cannot be predicted with the linearized analytical model. This implies that a linearized dimensional optimization is not accurate. This study has been carried out without any simplifying assumptions. Therefore, the calculations of the three magnetic field components are exact for all points in space, whatever the magnet dimensions. We can say that such a three-dimensional analytical approach is a good alternative to a finite element one because it has a lower computational cost and is more accurate.

Corresponding author: G. Lemarquand (guy.lemarquand@univ-lemans.fr).

## 1. INTRODUCTION

Nowadays, permanent magnets are widely used in electrical machines, motors or couplings because they offer very efficient solutions in terms of mechanical properties. Their magnetic energy density can commonly reach $560\,\mathrm{kJ}/m^3$. In addition, their coercive field and magnetic polarization allow one to use them in Halbach structures [1, 2]. As a consequence, some judicious assemblies of magnets have been studied in order to create either intense magnetic fields in the air gap or to optimize the radial field shape in electrical machines [3–5]. More generally, we can say that such structures allow us to obtain intense magnetic fields that are required for creating great torques in magnetic couplings. Several approaches can be used for studying the magnetic fields created by structures using permanent magnets. Among them, probably the most known for its versatility is the finite element method. Nevertheless, if the considered structure is completely three-dimensional with open boundaries, the accuracy of such numerical approaches can be questionable compared to an exact three-dimensional approach. Indeed, a high number of discretizing elements is required for precisely calculating the three components of the magnetic field. Consequently, two- and three-dimensional analytical approaches are good alternatives to this finite element method if their analytical calculation is possible. This is the case in ironless cylindrical structures. The interest of using analytical approaches is mainly due to their very low computational cost, easiness and accuracy. Indeed, such approaches allow us to easily realize parametric studies. The Halbach structure is a well-known configuration of magnets with alternate magnetizations. Many studies dealing with the optimization of such structures are based on two-dimensional analytical approaches. However, the accuracy of a linearized analytical model is questionable for studying alternate magnet structures when the permanent magnet dimensions are small, that is, when the curvature effect of the structure is important [6]. This is often the case when the radius of a cylindrical permanent magnet structure is small (typically inferior to 0.0025 m).

In this paper, we use the Coulombian model for determining the exact shape of the magnetic field produced by a Halbach structure. In addition, our approach allows us to study the accuracy of the linearized analytical approach generally used for optimizing Halbach structures. Furthermore, the three magnetic field components are determined without using any simplifying assumptions. This is also an important point because even if 2D or 3D linearized analytical models can be used for calculating the magnetic field created by such structures, some

effects cannot be predicted with these simplifying approaches and the accuracy of the results becomes questionable.

The expressions obtained are valid inside and outside the tile permanent magnet, whatever its dimensions. Consequently, we also discuss the effects of the demagnetizing field inside the tile permanent magnets. Moreover, the effects of all the magnetic pole contributions are discussed. The magnetic field created by tile permanent magnets can be determined analytically by using three-dimensional [7–22] and two-dimensional approaches [23–37]. In addition, the analytical expressions used for calculating the magnetic field produced by the tile permanent magnets have been published in previous papers [6, 39]. All the expressions determined in this paper are available online [40].

## 2. THE LINEARIZED ANALYTICAL MODEL OF A HALBACH STRUCTURE AND ITS LIMITS

### 2.1. Halbach Structure

This section presents an example of Halbach structure in Fig. 1 in which the tile permanent magnets are organized in order to have a rotating polarization of 90 degrees between two consecutive magnets. This was in fact the first structure proposed by Halbach. This choice is judicious because such a structure allows one to easily optimize the magnetic field shape in the air gap.

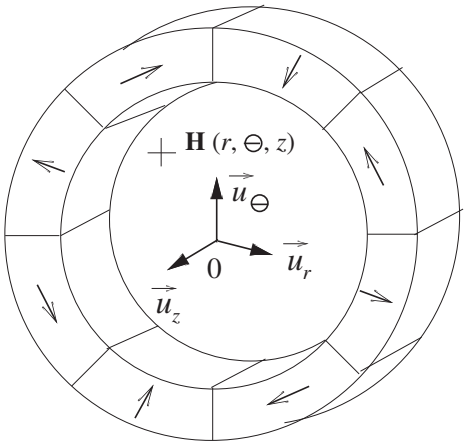


**Figure 1.** Representation of a cylindrical Halbach structure: an assembly of tile permanent magnets with different magnetizations.

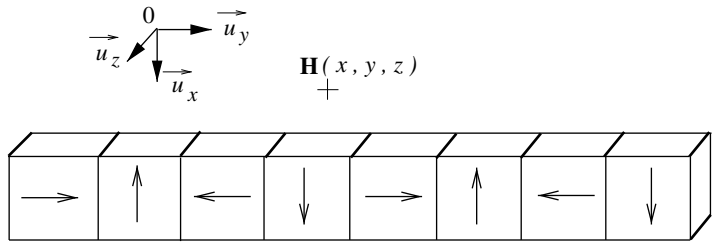


**Figure 2.** Representation of a linearized Halbach structure: an assembly of parallelepiped permanent magnets with different magnetizations.

### 2.2. Linearized Structure and Its Limits

Numerous analytical optimizations have been carried out by using a linearized configuration of the Halbach structure. This linearized configuration consists of an assembly of parallalelepiped permanent magnets with rotating polarizations as shown in Fig. 2. Consequently, the curvature effect of the alternate magnet structure is omitted. Nevertheless, the calculation of the three magnetic field components is fully analytical and the parametric optimization of such structures is thus simple to make. However, such an approach cannot be used when the curvature effect is important, that is, when the structure diameter is small. In addition, the linearized model turns out to be approximate when the angular width of the tile permanent magnets increases. Then, this linearized model cannot be used when the distance between the observation point and the magnet is high. Consequently, the far-field cannot be determined precisely with the linearized analytical model. As the tile permanent magnet polarizations are not perfectly radial or tangential, the linearized model cannot also forecast some effects that change the magnetic field shape. We propose in the next section to compare the magnetic field produced by a Halbach structure with our exact three-dimensional approach and the linearized approach.

## 3. THE MAGNETIC DIPPOLE REPRESENTATION FOR CALCULATING THE MAGNETIC FIELD PRODUCED BY THE LINEARIZED STRUCTURE

### 3.1. Basic Equation

The magnetic field produced by a linearized Halbach structure can be determined by using several analytical approaches. The most known analytical approach is certainly the magnetic dipole

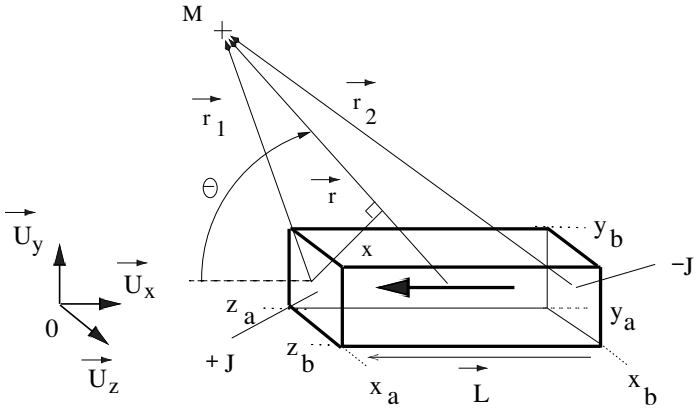


**Figure 3.** Permanent magnet with its dipole representation.

representation (Fig. 3). Such a representation is commonly used for calculating the external field **H** produced by a dipole source. According to this model, a permanent magnet is replaced by two magnetic poles which appear at the ends of the magnet. The interest of such an appraoch lies in the fact that its analytical expression is very simple. According to this model, the magnetic field $\mathbf{H}(\vec{r})$ produced by this permanent magnet is given by:

$$\mathbf{H}(\vec{r}) = \frac{JS}{4\pi\mu_0}\left(-\frac{\vec{r_1}}{r_1^3} + \frac{\vec{r_2}}{r_2^3}\right) \tag{1}$$

where $J$ is the magnetic charge of a magnetic pole and is expressed in tesla ($T$), $S$ is the surface of each extremity of the permanent magnet shown in Fig. 3 and $\mu_0$ is the permeability of the vacuum. All the other parameters are defined in Fig. 3. The well-known simplification consists in assuming that $\vec{L} \ll \vec{r}$. It leads us to write $\mathbf{H}(\vec{r})$ as follows:

$$\begin{aligned}\mathbf{H}(\vec{r}) \;=\; & \frac{JS}{4\pi\mu_0 r^3}\left[\left(-\frac{\vec{L}}{2} - \vec{r}\right)\left(1 - \frac{3L}{2r}\cos(\theta)\right)\right] \\ & + \frac{JS}{4\pi\mu_0 r^3}\left[\left(-\frac{\vec{L}}{2} + \vec{r}\right)\left(1 + \frac{3L}{2r}\cos(\theta)\right)\right]\end{aligned} \tag{2}$$

Eventually, we obtain the following expression:

$$\mathbf{H}(\vec{r}) = \frac{JV}{4\pi\mu_0 r^3}\left(-\hat{L} + 3(\hat{L}\cdot\hat{r})\hat{r}\right) \tag{3}$$

where $\hat{L} = \frac{\vec{L}}{L}$, $\hat{r} = \frac{\vec{r}}{r}$ and $V$ is the volume of the magnet. Eq. (3) is valid if the cross-section of the permanent magnet is small and if the observation point is determined far from the permanent magnet. We show in the next section that the optimization of a Halbach structure cannot be carried out by using this simplifying analytical method.

### 3.2. Accuracy of the Dipole Moment Representation in the Near-Field

We discuss here the accuracy of the dipole moment representation in the near-field, that is, near the permanent magnets. For this purpose, we use the exact three-dimensional analytical expression of the magnetic field produced by a permanent magnet. Let us consider the component $H_x$ of the magnetic field produced by a parallelepiped permanent magnet, as shown in Fig. 3. We note $H_x^{exact}$, the exact expression of this component and $H_x^{dipole}$ its simplifying analytical expression that is determined by (3). By using the notations shown in Fig. 3, the expression of $H_x^{exact}$ can be determined by using the Coulombian model with the following expression:

$$\begin{aligned} H_x^{exact} &= \frac{J}{4\pi\mu_0}\int_{y_a}^{y_b}\int_{z_a}^{z_b}\frac{(x-x_a)}{((x-x_a)^2+(y-\tilde{y})^2+(z-\tilde{z})^2)^{\frac{3}{2}}}d\tilde{y}d\tilde{z} \\ &\quad -\frac{J}{4\pi\mu_0}\int_{y_a}^{y_b}\int_{z_a}^{z_b}\frac{(x-x_b)}{((x-x_b)^2+(y-\tilde{y})^2+(z-\tilde{z})^2)^{\frac{3}{2}}}d\tilde{y}d\tilde{z} \end{aligned} \tag{4}$$

The integration of (4) leads to the analytical expression of $H_x^{exact}$ that is expressed as follows:

$$H_x^{exact} = f(x_a) - f(x_b) \tag{5}$$

where

$$\begin{aligned} f(x_i) &= \arctan\left[\frac{(y-y_a)(z-z_a)}{\xi(x_i,\, y_a,\, z_a)}\right] - \arctan\left[\frac{(y-y_b)(z-z_a)}{\xi(x_i,\, y_b,\, z_a)}\right] \\ &\quad - \arctan\left[\frac{(y-y_a)(z-z_b)}{\xi(x_i,\, y_a,\, z_b)}\right] + \arctan\left[\frac{(y-y_b)(z-z_b)}{\xi(x_i,\, x_b,\, z_b)}\right] \end{aligned} \tag{6}$$

where

$$\xi(x_i,\, y_i,\, z_i) = (x-x_i)\sqrt{(x-x_i)^2+(y-y_i)^2+(z-z_i)^2} \tag{7}$$

For performing our comparison, let us consider only the $x$-component of the magnetic field poduced by the parallelepiped magnet along the

$x$ direction. In this case, $H_x^{dipole}$ can be expressed as follows:

$$H_x^{dipole} = \frac{V}{x^3} \tag{8}$$

We define the difference $\Delta H_x$ as follows:

$$\Delta H_x = \left| H_x^{exact} - H_x^{dipole} \right| \tag{9}$$

where $V$ is the volume Therefore, we obtain:

$$\Delta H_x = \left| \frac{J}{4\pi\mu_0} \left( f(x_a) - f(x_b) - \frac{V}{x^3} \right) \right| \tag{10}$$

In addition, it is useful to define the relative difference $Dif$ as follows:

$$Dif = \left| \frac{H_x^{exact} - H_x^{dipole}}{H_x^{exact}} \right| \tag{11}$$

We represent this relative difference $Dif$ versus $x$ in Fig. 4. Figure 4

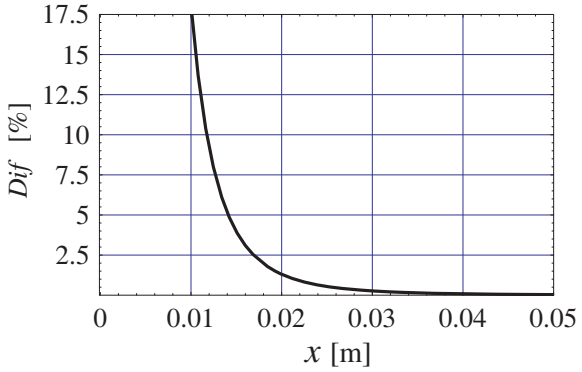


**Figure 4.** Representation of the relative difference $Dif$ versus $x$, the volume of the magnet is $V = 1\,\mathrm{cm}^3$ and its magnetic polarization $J$ equals 1 T, the middle of the magnet is placed in $x = 0$, the permanent magnet is cubic.

clearly shows that the well-known dipole model (3) cannot be used for studying the magnetic field produced by a tile permanent magnet. This difference is consistent with the assumptions taken for determining (3). We also see that the accuracy of the magnetic field expression with (3) remains questionable when the distance between the observation

point and the inner face of the magnet equals three times the $x$-length of the magnet (we incur an error of at least 4 per cent in this case). Consequently, we deduct that the optimization of a structure using tile permanent magnets must be carried out carefully if such a simplifying analytical model is used. Indeed, such a model is valid only in the far-field and cannot be used for optimizing the shape of the radial field of electrical machines or couplings. We propose now to compare the magnetic field produced by a Halbach structure and the one produced by its linearized structure.

## 4. USING THE COULOMBIAN MODEL FOR STUDYING THE HALBACH STRUCTURE

We present now the three dimensional analytical model that allows us to verify the accuracy of the linearized analytical model. Our three-dimensional model takes into account the curvature of the tile permanent magnets and all the surface densities located on the faces of each tile permanent magnet. As the considered magnets are uniformly magnetized, no magnetic pole volume densities appear in the magnets. As we use the Coulombian model for calculating the magnetic field for all points in space, each tile permanent magnet can be represented by some fictitious charge densities that are located on the faces of the magnet. However, these charges do not appear in the same way with the exact three dimensional model and with the linearized analytical model.

Figure 5(b) represents a tile permanent magnet radially magnetized and Fig. 5(a) its linearized structure. Thus, the curvature effect is omitted in the linearized structure and the fictitious magnetic poles appear only on two faces whereas they appear on the four faces of the magnet with the exact three-dimensional model. It is noted that the tile permanent magnets are supposed to be uniformly magnetized, as it is generally the case in practice. This implies that the magnetic field created by a tile permanent magnet radially magnetized is different from the one created by a parallelepiped permanent magnet, even in the near-field. For tile permanent magnets radially magnetized, we use the following notations: the radial field $H_{r,r}^{(3D)}$, the azimuthal field $H_{\theta,r}^{(3D)}$ and the axial field $H_{z,r}^{(3D)}$ are transfomed into $H_{x,r}^{(LIN)}$, $H_{y,r}^{(LIN)}$ and $H_{z,r}^{(LIN)}$ respectively.

Figure 6(b) represents a tile permanent magnet tangentially magnetized and Fig. 6(a) its linearized structure. Here again, the curvature effect is omitted in the linearized structure and the fictitious magnetic poles appear only on two faces for the linearized structure

whereas they appear on the four faces of the magnet for the exact three-dimensional model. For tile permanent magnets tangentially magnetized, we use the following notations: the radial field $H_{r,\theta}^{(3D)}$, the azimuthal field $H_{\theta,\theta}^{(3D)}$ and the axial field $H_{z,\theta}^{(3D)}$ are transformed into $H_{x,\theta}^{(LIN)}$, $H_{y,\theta}^{(LIN)}$ and $H_{z,\theta}^{(LIN)}$ respectively. In short, the magnetic field $\mathbf{H}(r,\,\theta,\,z)_r^{(3D)}$ produced by a tile permanent magnet radially magnetized is given by:

$$\mathbf{H}(r,\,\theta,\,z)_r^{(3D)} = H_{r,r}^{(3D)}\vec{u}_r + H_{\theta,r}^{(3D)}\vec{u}_\theta + H_{z,r}^{(3D)}\vec{u}_z \tag{12}$$

and the magnetic field $\mathbf{H}(x,\,y,\,z)_r^{(LIN)}$ produced by its linearized structure is given by:

$$\mathbf{H}(x,\,y,\,z)_r^{(LIN)} = H_{x,r}^{(LIN)}\vec{u}_x + H_{y,r}^{(LIN)}\vec{u}_y + H_{z,r}^{(LIN)}\vec{u}_z \tag{13}$$

In addition, the magnetic field $\mathbf{H}(r,\,\theta,\,z)_\theta^{(3D)}$ produced by a tile permanent magnet tangentially magnetized is given by:

$$\mathbf{H}(r,\,\theta,\,z)_\theta^{(3D)} = H_{r,\theta}^{(3D)}\vec{u}_r + H_{\theta,\theta}^{(3D)}\vec{u}_\theta + H_{z,\theta}^{(3D)}\vec{u}_z \tag{14}$$

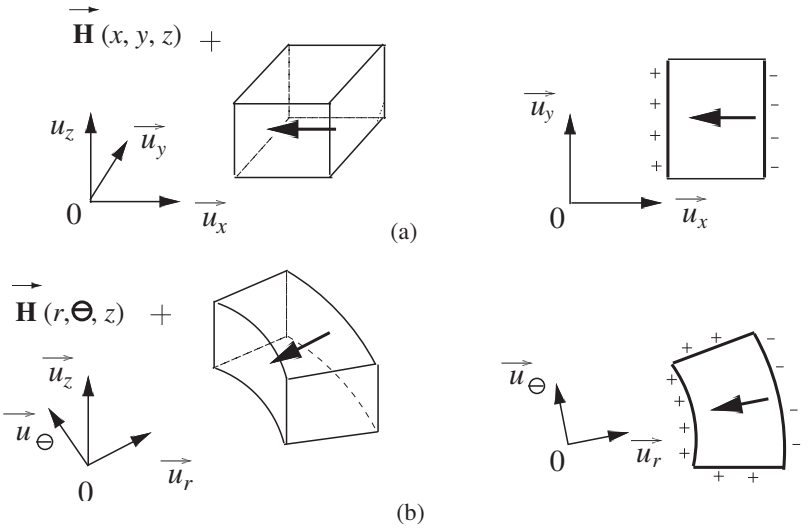


**Figure 5.** Representation of parallelepiped magnets whose polarization is directed along the $x$ axis and a tile permanent magnet radially magnetized.

and the magnetic field $\mathbf{H}(x,y,z)_{\theta}^{(\mathrm{LIN})}$ produced by its linearized structure is given by:

$$\mathbf{H}(x,\,y,\,z)_{\theta}^{(\mathrm{LIN})} = H_{x,\theta}^{(\mathrm{LIN})}\vec{u}_x + H_{y,\theta}^{(\mathrm{LIN})}\vec{u}_y + H_{z,\theta}^{(\mathrm{LIN})}\vec{u}_z \qquad (15)$$

Therefore, the linearized problem consists in determining $\mathbf{H}(x,y,z)_{r}^{(\mathrm{LIN})}$ and $\mathbf{H}(x,y,z)_{\theta}^{(\mathrm{LIN})}$ for calculating the magnetic field produced by an alternate magnet structure as shown in Fig. 1 by using the structure shown in Fig. 2. However, this linearized model is not accurate when the tile dimensions are small and do not forecast some phenomena that occur for tile permanent magnets whose polarization is tangential. As a consequence, a fully three-dimensional approach is required. The computational cost of the exact three-dimensional expressions is still very low compared to the finite element method one.

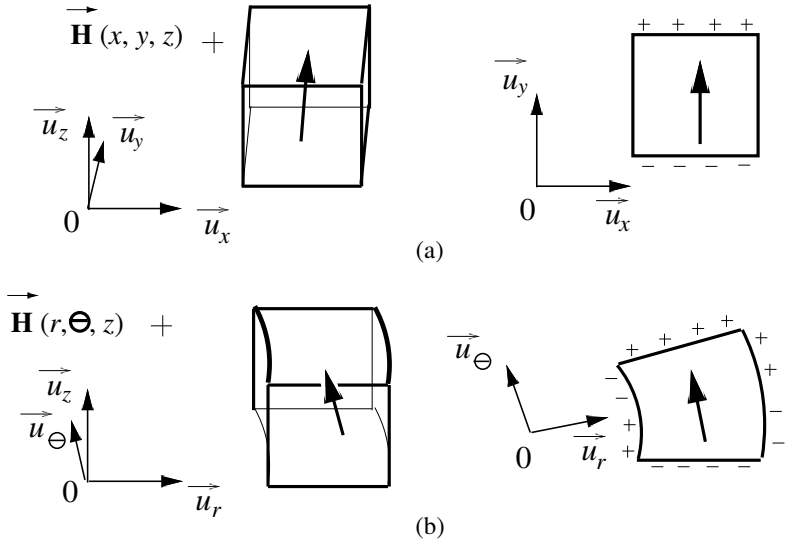


**Figure 6.** Representation of parallelepiped magnets whose polarization is directed along the $y$ axis and a tile permanent magnet tangentially magnetized.

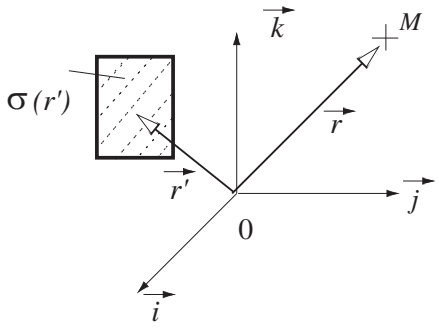


**Figure 7.** Magnetic pole distribution creating a magnetic field at a given observation point $M$.

### 4.1. Calculating the Magnetic Field Created by a Magnetic Pole Surface Density

For each configuration studied in this paper, the magnetic field components are determined by using the Coulombian Model. Consequently, the magnetic component $H_i$ created by one permanent magnet is always determined analytically by using the following equation:

$$H_i = \mathbf{H} \cdot \vec{u}_i = \vec{\nabla} \left( \frac{1}{4\pi\mu_0} \iint_S G(\vec{r}, \vec{r'}) \sigma(\vec{r'}) dS \right) \cdot \vec{u}_i \tag{16}$$

where $\mu_0$ is the permeability of the vacuum and $G(\vec{r}, \vec{r'})$ is the Green's function defined by

$$G(\vec{r}, \vec{r'}) = \frac{1}{\left| \vec{r} - \vec{r'} \right|} \tag{17}$$

and the vectors $\vec{r}$ and $\vec{r'}$ are shown in Fig. 7. In short, the magnetic component $H_i$ at a given observation point $M$ is always determined analytically by using the Coulombian Model. In our case, as our structure is ironless, we can use either the three-dimensional Green's function or directly the Coulombian Model for calculating the three magnetic components for all points in space. In addition, it is noted that no magnetic pole volume densities appear because the permanent magnets used are uniformly magnetized. All the analytical expressions used in this paper are presented in the appendix.

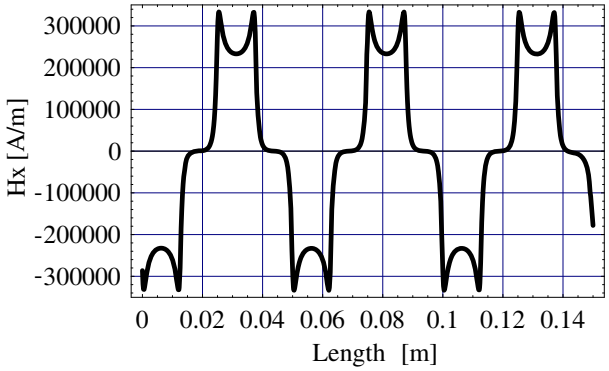


**Figure 8.** Normal field created by a linearized Halbach structure versus the length $y$, the radial distance equals 0.5 mm from the magnets, $x_a = 0.025\,\mathrm{m}$, $x_b = 0.028\,\mathrm{m}$, $J = 1\,\mathrm{T}$, $h = 0.003\,\mathrm{m}$, $z = 0.0015\,\mathrm{m}$.

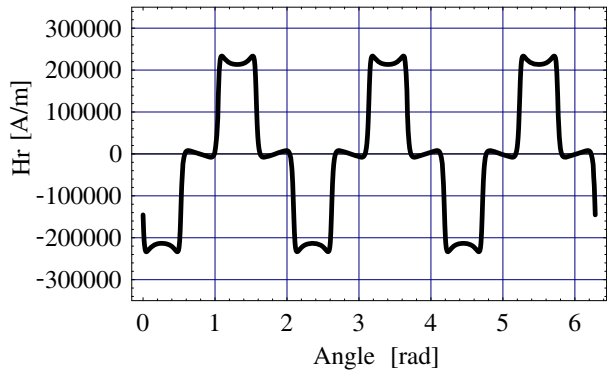


**Figure 9.** Radial field created by a Halbach structure versus the angle $\theta$, the radial distance equals 0.5 mm from the magnets, $r_{\mathrm{in}} = 0.025\,\mathrm{m}$, $r_{\mathrm{out}} = 0.028\,\mathrm{m}$, $h = 0.003\,\mathrm{m}$, $J = 1\,\mathrm{T}$, $z = 0.0015\,\mathrm{m}$.

## 5. RADIAL FIELD CREATED BY A HALBACH STRUCTURE

### 5.1. Comparison between the Linearized Approach and Our Three-Dimensional Approach

Several analytical studies have been carried out for optimizing the tile permanent magnet dimensions so as to obtain the intended radial field. We represent in Figs. 8 and 9 the radial field produced by a Halbach structure whose magnets have the same angular widths ($\theta_{width} = \frac{\pi}{6}$).

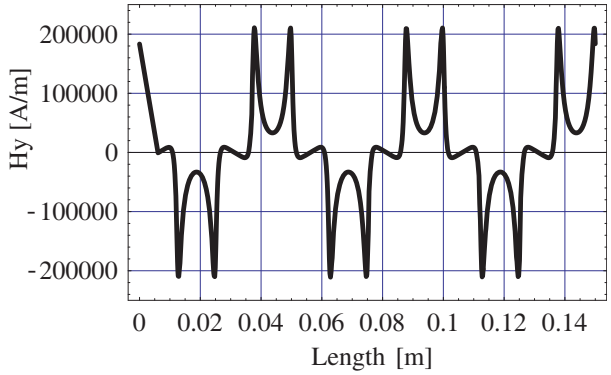


**Figure 10.** Perpendicular field created by a linearized Halbach structure versus the length of the linearized structure, the radial distance equals 0.5 mm from the magnets, $x_a = 0.025$ m, $x_b = 0.028$ m, $J = 1$ T, $h = 0.003$ m, $z = 0.0015$ m.

For the tile permanent magnet, the inner radius $r_{in}$ is 0.025 m; the outer one $r_{out}$ equals 0.028 m; its height is $h = 0.003$ m. For the parallelepiped magnet, the inner radius $x_a$ is 0.025 m; the outer one $x_b$ equals 0.028 m; its height is $h = 0.003$ m. These dimensions are the same for all the simulations. Each tile permanent magnet has a radial width that equals 0.003 m. The angular width in the linearized structure becomes merely a length that equals $r_{in}\theta_{width}$. Figures 8 and 9 show that both the shape and the value of radial field are different when they are calculated close to the magnets. These differences can be explained by investigating the way the fictitious magnetic pole surface densities are located on the faces of the magnets. Fig. 6(a) shows that the linearized structure has not the same repartition of fictitious magnetic pole surface densities as the Halbach structure shown in Fig. 6(b). Some positive charges appear on only one side of a magnet with the linearized structure whereas they appear on three sides of the magnet in a tile magnet tangentially magnetized. This is in fact an important point because it allows us to optimize the tile permanent magnet dimensions in order to minimize the effect of the fictitious magnetic charges located on the arc-shaped faces of the magnet. Such an optimization cannot be carried out with a linearized structure. The shape and the values of the radial field are consistent with the interpretation of Figs. 6(a) and 6(b). The normal field determined with the linearized structure is over-estimated because the magnetic charges located on the arc-shaped faces of the magnet are omitted.

### 5.2. Influence on the Electromotive Force in an Electrical Machine

We discuss here qualitatively another phenomenon that cannot be predicted with the linearized approach. Indeed, in electrical machines, an important parameter is the electromotive force that is defined by:

$$e_m = -\frac{d\Phi}{dt} \tag{18}$$

or, by using the notations of this paper,

$$e_m = -\mu_0 \frac{d}{dt} \iint_{(S_j)} \vec{\nabla} \left( \frac{1}{4\pi\mu_0} \iint_{S_i} G(\vec{r}, \vec{r'}) \sigma(\vec{r'}) dS_i \right) \cdot d\vec{S_j} \tag{19}$$

where $S_i$ is the surface of the tile permanent magnets in the first rotor and $S_j$ is the surface of the tile permanent magnets in the second rotor. We consider here only two faces for simplifying (16). We deduct that the radial field changes its sign with respect to the variation of $\theta$ more often with the three-dimensional approach than the linearized approach, as shown in Figs. 8 and 9. This generates harmonics that lower the quality of the electrical machines. Consequently, if electrical machines are optimized by using only the linearized model, this behaviour cannot be predicted.

## 6. TANGENTIAL FIELD CREATED BY A HALBACH STRUCTURE

Let us now consider the tangential field created by a Halbach structure. Such a magnetic field is also interesting to study because it is used for calculating magnetic couplings or the demagnetizing field inside the tile permanent magnets. As stated previously, the shape of the azimuthal field is different between the Halbach structure and its linearized configuration. We represent in Figs. 11 and 12 the azimuthal field created by the Halbach structure described in Fig. 2 and Fig. 1. The radial observation point is calculated at a distance which equals 0.5 mm from the magnets. Here again, we see that several differences appear between the azimuthal field calculated with the exact three-dimensional approach and the linearized approach. The most important difference is clearly the shape of the azimuthal field that is not well described with the linearized approach. It can be explained by the transition between two consecutive parallelepiped magnets, which generates a change in the sign of the azimuthal component, that is, $H_{y,r}^{(\mathrm{LIN})}$ and $H_{y,\theta}^{(\mathrm{LIN})}$. However, strictly speaking,

the total sum of the charges generate merely a smooth variation of this transition between $H_{r,r}^{(3D)}$ and $H_{r,\theta}^{(3D)}$. Consequently, the optimization of this component cannot be carried out accurately with the linearized approach in the near field.

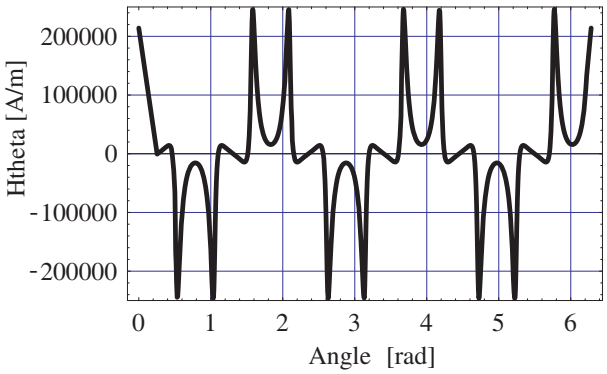


**Figure 11.** Azimuthal field created by a Halbach structure versus the angle $\theta$, the radial distance equals 0.5 mm from the magnets, $r_{\text{in}} = 0.025\,\text{m}$, $r_{\text{out}} = 0.028\,\text{m}$, $h = 0.003\,\text{m}$, $J = 1\,\text{T}$, $z = 0.0015\,\text{m}$.

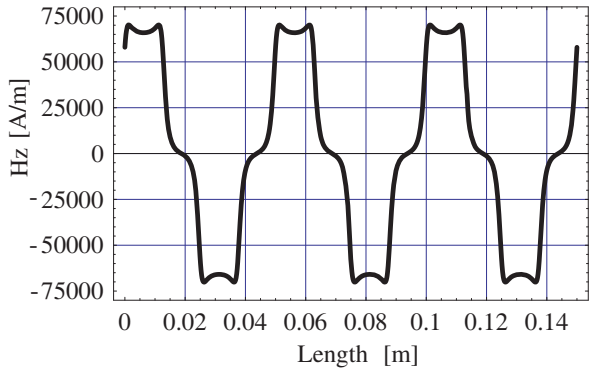


**Figure 12.** Axial field created by a linearized Halbach structure versus the length of the linearized structure, the radial distance equals 0.5 mm from the magnets, $x_a = 0.025\,\text{m}$, $x_b = 0.028\,\text{m}$, $J = 1\,\text{T}$, $h = 0.003\,\text{m}$, $z = 0.0015\,\text{m}$.

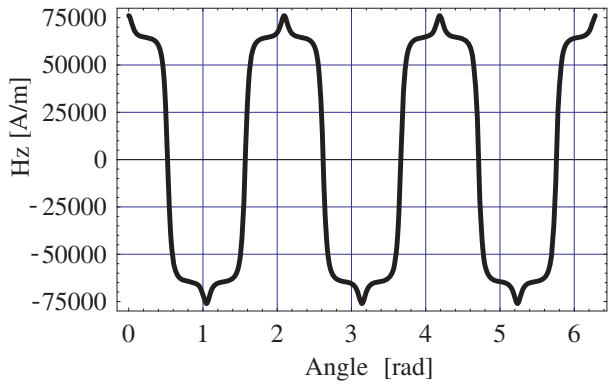


**Figure 13.** Axial field created by a Halbach structure versus the angle $\theta$, the radial distance equals 0.5mm from the magnets, $r_{\text{in}} = 0.025\,\text{m}$, $r_{\text{out}} = 0.028\,\text{m}$, $h = 0.003\,\text{m}$, $J = 1\,\text{T}$, $z = 0.0015\,\text{m}$.

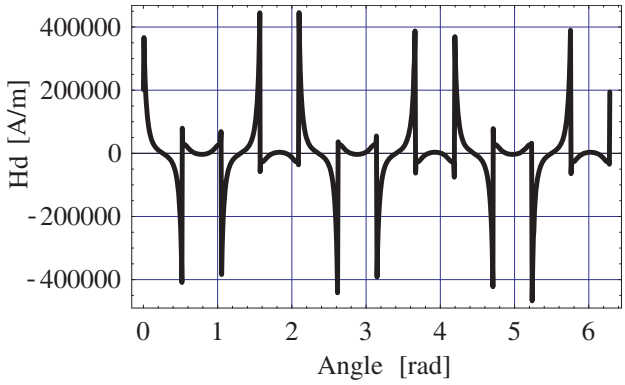


**Figure 14.** Representation of the azimuthal component of the demagnetizing field $H_\theta$ inside the tile permanent magnets versus the angle $\theta$, the radial distance equals 0.2 mm from the inner faces of the tile permanent magnets, $r_{\text{in}} = 0.025\,\text{m}$, $r_{\text{out}} = 0.028\,\text{m}$, $h = 0.003\,\text{m}$, $J = 1\,\text{T}$, $z = 0.0015\,\text{m}$.

## 7. AXIAL FIELD CREATED BY A HALBACH STRUCTURE

Let us now consider the axial field created by a Halbach structure. This component is of great importance in ironless motors with ferrofluid seals in which the accurate knowledge of these values allows us to

optimize the ferrofluid seals. First, we study the axial magnetic field in the near field, that is, for a radial observation point which equals 0.5 mm from the magnets. We represent in Figs. 13 and 14 the axial component with the exact three-dimensional approach and the linearized approach. Figs. 13 and 14 show that the value of the axial field is rather well determined with the linearized approach. However, the shape of this axial component is different. This is typically the case when the linearized approach cannot be used for studying the shape of the axial field produced by an assembly of tile permanent magnets. Indeed, the shape of the axial field is inverted at the maxima between the exact three-dimensional approach and the linearized approach. Indeed, the shape of the axial field is inverted at the maxima between the exact three-dimensional approach and the linearized.

## 8. DETERMINATION OF THE DEMAGNETIZING FIELD H INSIDE THE TILE PERMANENT MAGNETS

We discuss here the behaviour of the demagnetizing field **H** inside the tile permanent magnets. Strictly speaking, there are three components that define this demagnetizing field. However, the azimuthal component is the most important one that plays a role in the demagnetization of a tile permanent magnet in an Halbach structure. This component is denoted $H_\theta$. It must be emphasized that the total demagnetizing field in a tile permanent magnet is the sum of its own

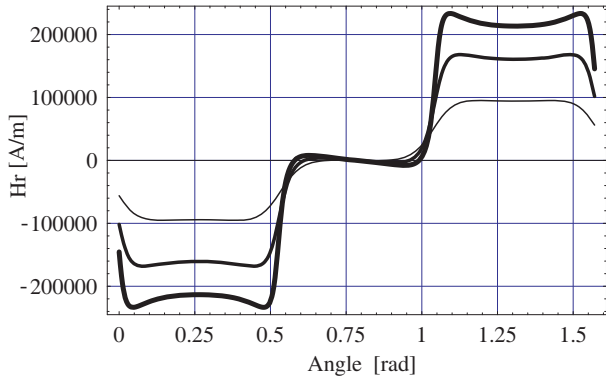


**Figure 15.** Representation of the radial component versus $\theta$ for three radial observation points ($r = 0.0245\,\mathrm{m}$, $r = 0.024\,\mathrm{m}$, $r = 0.023\,\mathrm{m}$), $r_{\mathrm{in}} = 0.025\,\mathrm{m}$, $r_{\mathrm{out}} = 0.028\,\mathrm{m}$, $h = 0.003\,\mathrm{m}$, $J = 1\,\mathrm{T}$, $z = 0.0015\,\mathrm{m}$, the more the radial field is determined far from the magnets, the more the line is thicker.

demagnetizing field and the demagnetizing field produced by the other tile permanent magnets. In a Halbach structure, a tile permanent magnet can be demagnetized because of the value of $H_\theta$ near the corners of the tile permanent magnets. This behaviour can be predicted by using our three-dimensional analytical model. For this purpose, we represent in Fig. 15 the total demagnetizing field $H_\theta$ versus the angle $\theta$. Fig. 15 clearly shows that $H_\theta$ reaches very high values when the $\theta$ is near the transition between two consecutive magnets. At each transition, we have $H_\theta = 420000\,\mathrm{A/m}$ while the observation point is not strictly located on the faces of the tile permanent magnets. This signifies that the magnet undergoes a very high magnetic field near its corners and it can probably be slightly demagnetized. Consequently, it can generate for example a decrease in the value of the torque in magnetic couplings. As these effects must be carefully studied in a parametric optimization of such structures, the approach taken must be both accurate and fast. This is the case with our three-dimensional analytical approach.

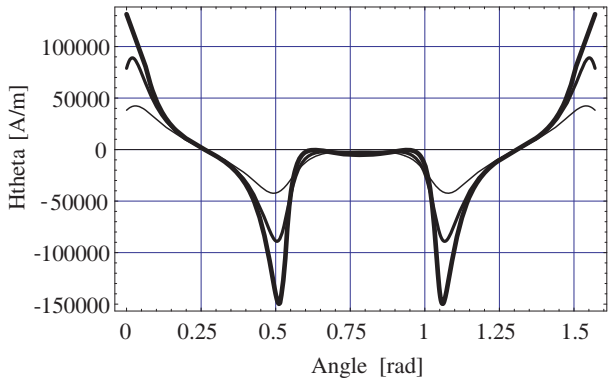


**Figure 16.** Representation of the azimuthal component versus $\theta$ for three radial observation points ($r = 0.0245\,\mathrm{m}$, $r = 0.024\,\mathrm{m}$, $r = 0.023\,\mathrm{m}$), $r_{\mathrm{in}} = 0.025\,\mathrm{m}$, $r_{\mathrm{out}} = 0.028\,\mathrm{m}$, $h = 0.003\,\mathrm{m}$, $J = 1\,\mathrm{T}$, $z = 0.0015\,\mathrm{m}$, the more the radial field is determined far from the magnets, the more the line is thicker.

## 9. DEFORMATION OF THE MAGNETIC FIELD IN A HALBACH STRUCTURE

### 9.1. Deformation of the Radial Field according to the Radial Observation Point

We illustrate in this section the way the magnetic field shape changes according to the radial observation point by using our exact three-dimensional approach. This element of information is important for the design of electrical machines because the shape of the radial field greatly influences the voltage delivered by the electrical machine. As the optimization of the shape of the radial field is often carried out with the linearized structure, some effects cannot be predicted accurately. Consequently, the dimensions of the inner rotor of an electrical machine must be carefully optimized for avoiding these distortions. We represent in Fig. 16 the radial field created by an assembly of tile permanent magnets. We take the following dimensions: $r_{\text{in}} = 0.025\,\text{m}$, $r_{\text{out}} = 0.028\,\text{m}$, $h = 0.003\,\text{m}$, $J = 1\,\text{T}$, $z = 0.0015\,\text{m}$. In addition, the farther the radial field is from the magnets, the thicker is the line in Fig. 16. In this representation, we take respectively $r = 0.0245\,\text{m}$, $r = 0.024\,\text{m}$ and $r = 0.023\,\text{m}$. The most important phenomenon in Fig. 16 that can be predicted only with our three-dimensional appraoch is the deformation of the radial field shape. Indeed, when the radial field is far from the magnets (the thinner line), the radial field shape is smoother than when it is calculated far from the magnets (the thicker line). Thus, the air gap and the number of tile permanent magnets used have a great influence on the quality of an electrical machine. These parameters can be optimized by using an exact three dimensional approach.

### 9.2. Deformation of the Azimuthal Field according to the Radial Observation Point

Our exact analytical three-dimensional approach is useful for studying the deformation of the azimuthal field produced by a Halbach structure according to the radial observation point. Such a calculation is required for optimizing the torque transmitted in magnetic couplings. Up to now, such studies have been carried out by using only the linearized models [31–33]. However, these linearized models are not sufficient for accurately optimizing the air gap dimensions in order to obtain the great torque in magnetic couplings. We represent in Fig. 17 the azimuthal field produced by a Halbach structure with the following dimensions: $r_{\text{in}} = 0.025\,\text{m}$, $r_{\text{out}} = 0.028\,\text{m}$, $h = 0.003\,\text{m}$, $J = 1\,\text{T}$, $\theta_{\text{width}} = \frac{\pi}{6}$ and with the three following radial observation points

$r = 0.0245\,\mathrm{m}$, $r = 0.024\,\mathrm{m}$ and $r = 0.023\,\mathrm{m}$. Fig. 17 confirms that both the value and the shape of the azimuthal field depend greatly on the radial observation point. This implies that the analytical optimization of a structure using tile permanent magnets must be carried out with exact three-dimensional expressions.

## 10. THREE-DIMENSIONAL OPTIMIZATION OF A CYLINDRICAL HALBACH STRUCTURE

We present now an optimization of a cylindrical Halbach structure for permanent magnet machines. Basically, there are two kinds of permanent magnet machines. The first one creates a radial field whose shape is perfectly sinusoidal whereas the second type generates radial field whose shape is a trapezoid. We propose two optimizations of these devices with always the same radial observation point.

### 10.1. Permanent Magnet Machines Generating Sinusoidal Radial Fields

We propose here an optimized Halbach structure obtained with our three dimensional analytical approach. The aim of this Halbach structure is to create a radial field whose shape is sinusoidal. Let us consider a Halbach structure with 24 pairs of tile permanent magnets.

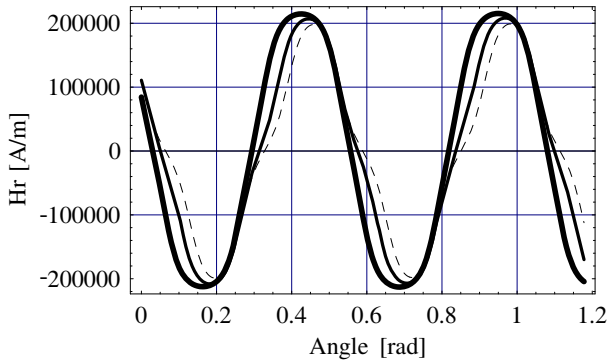


**Figure 17.** Representation of the radial field versus $\theta$ produced by an optimized Halbach structure. $r = 0.024\,\mathrm{m}$, $r_{\mathrm{in}} = 0.025\,\mathrm{m}$, $r_{\mathrm{out}} = 0.028\,\mathrm{m}$, $h = 0.003\,\mathrm{m}$, $J = 1\,\mathrm{T}$, $z = 0.0015\,\mathrm{m}$, (thick line: the angular width ratio between the tile permanent magnets radially and tangentially magnetized is $\frac{1}{3}$), (thin line: the ratio is $\frac{3}{2}$), (dashed line: the ratio is 1).

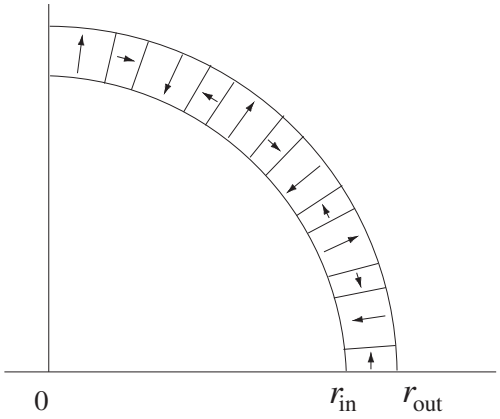


**Figure 18.** Representation of the optimized Halbach structure that creates a radial field whose shape is sinusoidal with the following dimensions: $r = 0.024\,\mathrm{m}$, $r_{in} = 0.025\,\mathrm{m}$, $r_{out} = 0.028\,\mathrm{m}$, $h = 0.003\,\mathrm{m}$, $J = 1\,\mathrm{T}$, $z = 0.0015\,\mathrm{m}$ and 24 pairs of tile permanent magnets. The ratio between the tile permanent magnets radially and tangentially magnetized is $\frac{1}{3}$.

We represent in Fig. 19 the corresponding Halbach structure that creates a radial field whose shape is sinusoidal. The inner radius of the Halbach structure equals 0.025 m and the outer one equals 0.028 m. In addition, we take $h = 0.003\,\mathrm{m}$ and $z = 0.0015\,\mathrm{m}$. The radial field is optimized at a distance that equals 0.001 m from the tile permanent magnets. Therefore, we take $r = 0.024\,\mathrm{m}$. By using our three dimensional approach, we find a good compromise between the angular widths of the tile permanent magnets radially and tangentially magnetized. We represente in Fig. 17 three representations of the radial field versus the angular distance with the following ratios between the angular widths of the tile permanent magnets radially or tangentially magnetized: 1, $\frac{3}{2}$ and 3. We find that a best compromise can be found when the ratio equals 3 between the tile permanent magnets radially and tangentially magnetized.

### 10.2. Permanent Magnet Machines Generating Trapezoid Radial Fields

We propose here an optimized Halbach structure that creates a radial field whose shape is a trapezoid. Let us consider a Halbach structure with 16 pairs of tile permanent magnets. The inner radius of the Halbach structure equals 0.025 m and the outer one equals 0.028 m.

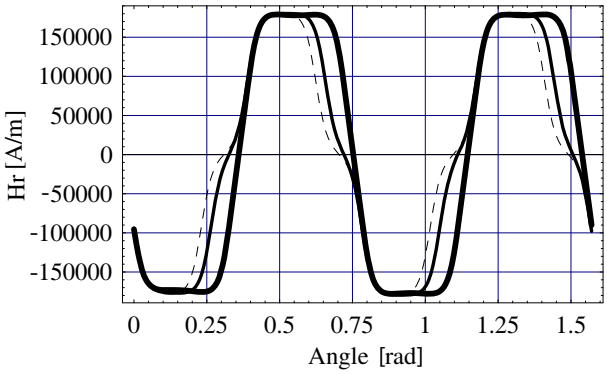


**Figure 19.** Representation of the radial field versus $\theta$ produced by an optimized Halbach structure. $r = 0.024\,\mathrm{m}$, $r_{\mathrm{in}} = 0.025\,\mathrm{m}$, $r_{\mathrm{out}} = 0.028\,\mathrm{m}$, $h = 0.003\,\mathrm{m}$, $J = 1\,\mathrm{T}$, $z = 0.0015\,\mathrm{m}$. (Thick line: the angular width ratio between the tile permanent magnets radially and tangentially magnetized is $\frac{1}{5}$), (thin line: the ratio is $\frac{1}{2}$), (dashed line: the ratio is $\frac{5}{6}$).

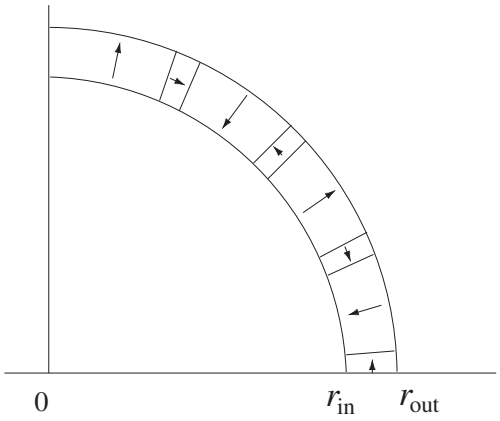


**Figure 20.** Representation of the optimized Halbach structure that creates a radial field whose shape is a trapezoid with the following dimensions: $r = 0.024\,\mathrm{m}$, $r_{\mathrm{in}} = 0.025\,\mathrm{m}$, $r_{\mathrm{out}} = 0.028\,\mathrm{m}$, $h = 0.003\,\mathrm{m}$, $J = 1\,\mathrm{T}$, $z = 0.0015\,\mathrm{m}$ and 16 pairs of tile permanent magnets. The ratio between the tile permanent magnets radially and tangentially magnetized is $\frac{1}{5}$.

In addition, we take $h = 0.003\,\mathrm{m}$ and $z = 0.0015\,\mathrm{m}$. The radial field is optimized at a distance that equals $0.001\,\mathrm{m}$ from the tile permanent magnets. Therefore, we take $r = 0.024\,\mathrm{m}$. We have represente in Fig. 19 three representations of the radial field versus the angular distance with the following ratios between the angular widths of the tile permanent magnets radially or tangentially magnetized: $\frac{1}{5}$, $\frac{1}{2}$ and $\frac{5}{6}$. We find that a best compromise can be found when the ratio equals $\frac{1}{5}$ between the tile permanent magnets radially and tangentially magnetized. We represent in Fig. 20 the corresponding Halbach structure that creates a radial field whose shape is a trapezoid.

## 11. CONCLUSION

This paper has presented the exact shape of the magnetic field produced by a Halbach structure by using the Coulombian model. This approach allowed us to discuss the accuracy of the linearized model for studying the three magnetic components in the air gap. Some phenomena cannot be predicted with the linearized approach whereas they can be determined accurately with a three dimensional approach without using any simplifying assumptions. The time necessary to optimize tile permanent magnets remains very low compared to the one of the finite-element method. Moreover, such an approach can be used to verify the accuracy of a classical finite-element method. We have also presented the interest of using such an approach by studying the demagnetizing field inside the tile permanent magnets. This element of information is important for the design of Halbach structures. Eventually, we have illustrated our three-dimensional approach with two optimized Halbach structures that create radial fields with required shapes. We have proposed two kinds of structures. The first one corresponds to a Halbach structure that creates a radial field whose shape is sinusoidal. The second one corresponds to a Halbach structure whose shape is a trapezoid.

## APPENDIX A. ANALYTICAL EXPRESSIONS OF THE MAGNETIC FIELD CREATED BY TILE PERMANENT MAGNETS

### A.1. Tile Permanent Magnets Uniformy and Tangentially Magnetized

We give here the analytical expressions of the magnetic field created by tile permanent magnets whose polarization is both uniform and tangential.

For this purpose, the geometry and the related parameters are shown in Fig. 21. The radial component of the magnetic field created

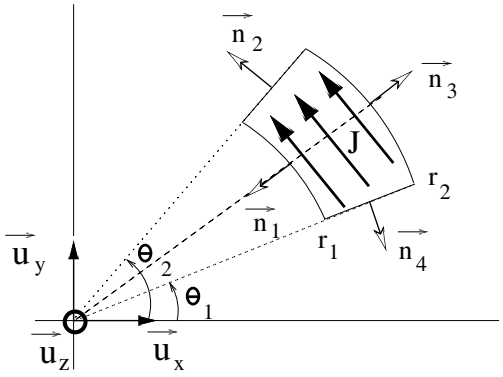


**Figure 21.** Representation of the geometry considered. The tile inner radius is $r_1$, the tile outer radius is $r_2$, its angular width is $\theta_2 - \theta_1$. Its magnetic polarization is $\vec{J}$. In addition, the height is $z_2 - z_1$

by a tile permanent magnet whose polarization is both uniform and tangential can be expressed as follows:

$$\begin{aligned} H_r(r,\theta,z) &= \sum_{i=1}^{2}\sum_{j=1}^{2}(-1)^{(i+j)}h_r^{(I)}(r_i,z_j) \\ &\quad + \sum_{i=1}^{2}\sum_{j=1}^{2}\sum_{k=1}^{2}(-1)^{(i+j+k)}h_r^{(II)}(r_i,z_j,\theta_k) \end{aligned} \tag{A1}$$

where $h_r^{(I)}(r_i,z_j)$ represents the magnetic field created by the fictitious magnetic poles located on the arc-shaped faces of the tile permanent magnet and $h_r^{(II)}(r_i,z_j,\theta_k)$ represents the magnetic field created by the fictitious magnetic poles located on the straight faces of the tile permanent magnet.

$$h_r^{(I)}(r_i,z_j) = \frac{J}{4\pi\mu_0}r_i(z-z_j)\tilde{\mathbf{E}}^*\left[\theta_a,r_i,z_j\right] \tag{A2}$$

$$\begin{aligned} h_r^{(II)}(r_i,z_j,\theta_k) &= -\frac{J\cos(\frac{\theta_1-\theta_2}{2})}{8\pi\mu_0 X_k}\left((1-x_k^2+x_kX_k)\log[A_{i,j,k}]\right) \\ &\quad -\frac{J\cos(\frac{\theta_1-\theta_2}{2})}{8\pi\mu_0 X_k}\left((-1+x_k^2+x_kX_k)\log[B_{i,j,k}]\right) \end{aligned} \tag{A3}$$

where $\tilde{\mathbf{E}}^* [\theta_a, r_i, z_j]$ can be seen as a non-classical elliptic integral that is defined as follows:

$$\tilde{\mathbf{E}}^* [\theta_a, r_i, z_j] = \int_{\theta_1}^{\theta_2} \frac{(r - r_i \cos(\theta - \tilde{\theta})) \sin(\theta_a - \tilde{\theta})}{\xi(i, j, \tilde{\theta}) \left( \xi(i, j, \tilde{\theta})^2 - (z - z_j)^2 \right)} d\tilde{\theta} \tag{A4}$$

and

$$\begin{aligned} A_{i,j,k} \;=\; & \frac{2(r r_i X_k^2 + r^2 X_k^2 (-x_k + X_k))}{(-X_k^2 + x_x X_k)(r_i + r(-x_k + X_k))(z - z_j)} \\ & - \frac{2X_k (z - z_j + \sqrt{r^2 + r_i^2 - 2 r r_i x_k + (z - z_j)^2})}{(-X_k^2 + x_x X_k)(r_i + r(-x_k + X_k))} \end{aligned} \tag{A5}$$

$$\begin{aligned} B_{i,j,k} \;=\; & - \frac{2(r r_i X_k^2 - r^2 X_k^2 (x_k + X_k))}{(X_k^2 + x_k X_k)(r_i - r(x_k + X_k))(z - z_j)} \\ & + \frac{2X_k (z - z_j + \sqrt{r^2 + r_i^2 - 2 r r_i x_k + (z - z_j)^2})}{(X_k^2 + x_k X_k)(r_i - r(x_k + X_k))} \end{aligned} \tag{A6}$$

with

$$X_k = \sqrt{x_k^2 - 1} = \sqrt{\cos(\theta - \theta_k)^2 - 1} \tag{A7}$$

and

$$\xi(i, j, \theta_k) = \sqrt{r^2 + r_i^2 + (z - z_j)^2 - 2 r r_i \cos(\theta - \theta_k)} \tag{A8}$$

It is emphasized here that $h_r^{(II)}(r_i, z_j, \theta_k)$ is fully analytical whereas $h_r^{(I)}(r_i, z_j)$ is based on a non-classical elliptic integral. The azimuthal component of the magnetic field created by a tile permanent magnet whose polarization is both uniform and tangential is expressed as follows:

$$\begin{aligned} H_\theta(r, \theta, z) \;=\; & \sum_{i=1}^{2} \sum_{j=1}^{2} (-1)^{(i+j)} h_\theta^{(I)}(r_i, z_j) \\ & + \sum_{i=1}^{2} \sum_{j=1}^{2} \sum_{k=1}^{2} (-1)^{(i+j+k)} h_\theta^{(II)}(r_i, z_j, \theta_k) \end{aligned} \tag{A9}$$

with

$$h_\theta^{(I)}(r_i, z_j) = \frac{J}{4\pi\mu_0} r_i^2 (z - z_j) \tilde{\mathbf{L}}^* \left[ \frac{\theta_1 + \theta_2}{2}, r_i, z_j \right] \tag{A10}$$

where $\tilde{\mathbf{L}}^*[\theta_a, r_i, z_j]$ can be seen as a non classical definite elliptic integral.

$$\tilde{\mathbf{L}}^*[\theta_a, r_i, z_j] = \int_{\theta_1}^{\theta_2} \frac{\sin(\theta_a - \tilde{\theta})\sin(\theta - \tilde{\theta})}{\xi(i,j,\tilde{\theta})\left(\xi(i,j,\tilde{\theta})^2 - (z - z_j)^2\right)} d\tilde{\theta} \tag{A11}$$

and

$$\begin{aligned} h_\theta^{(II)}(r_i, z_j, \theta_k) = & \frac{J\cos(\frac{\theta_1-\theta_2}{2})}{8\pi\mu_0} \frac{2r + y_k\left(-x_k + \tilde{X_k}\right)}{\tilde{X_k}} \log\left[C_{i,j,k}\right] \\ & + \frac{J\cos(\frac{\theta_1-\theta_2}{2})}{8\pi\mu_0} \frac{-2r + y_k\left(x_k + \tilde{X_k}\right)}{\tilde{X_k}} \log\left[D_{i,j,k}\right] \end{aligned} \tag{A12}$$

$$\begin{aligned} C_{i,j,k} = & \frac{4\tilde{X_k}\left((z_j - z) - \sqrt{r^2 + r_i^2 - r_i\tilde{x_k} + (z - z_j)^2}\right)}{(2r_i - \tilde{x_k} + \tilde{X_k})\left(2r + (X_k \tilde{-} \tilde{x_k})y_k\right)} \\ & + \frac{\tilde{X_k}(\tilde{x_k}^2 - 4r^2) + (2r_i - \tilde{x_k})(\tilde{x_k}^2 - 4r^2)}{(2r_i - \tilde{x_k} + \tilde{X_k})\left(2r + (X_k \tilde{-} \tilde{x_k})y_k\right)(z - z_j)} \end{aligned} \tag{A13}$$

$$\begin{aligned} D_{i,j,k} = & \frac{4\tilde{X_k}\left(\sqrt{r^2 + r_i^2 - r_i\tilde{x_k} + (z - z_j)^2} + (z - z_j)\right)}{(-2r_i + \tilde{x_k} + \tilde{X_k})\left(-2r + (\tilde{x_k} + \tilde{X_k})y_k\right)} \\ & + \frac{\left(4r^2 - \tilde{x_k}^2\right)}{\left(-2r + (\tilde{x_k} + \tilde{X_k})y_k\right)(z - z_j)} \end{aligned} \tag{A14}$$

with

$$\tilde{X_k} = \sqrt{\tilde{x_k}^2 - 4r^2} = \sqrt{(2r\cos(\theta - \theta_k))^2 - 4r^2} \tag{A15}$$

$$y_k = \sin(\theta - \theta_k) \tag{A16}$$

The axial component $H_z(r, \theta, z)$ can be expressed as follows:

$$\begin{aligned} H_z(r, \theta, z) = & \sum_{i=1}^{2}\sum_{j=1}^{2}(-1)^{(i+j)} h_z^{(I)}(r_i, z_j) \\ & + \sum_{i=1}^{2}\sum_{j=1}^{2}\sum_{k=1}^{2}(-1)^{(i+j+k)} h_z^{(II)}(r_i, z_j, \theta_k) \end{aligned} \tag{A17}$$

with

$$h_z^{(I)}(r_i, z_j) = \frac{J}{4\pi\mu_0}(-r_i)\tilde{\mathbf{K}}^* \left[\frac{\theta_1 + \theta_2}{2}, r_i, z_j\right] \tag{A18}$$

where $\tilde{\mathbf{K}}^* [\theta_a, r_i, z_j]$ represents a non-classical definite elliptic integral that is defined as follows:

$$\tilde{\mathbf{K}}^* [\theta_a, r_i, z_j] = \int_{\theta_1}^{\theta_2} \frac{\sin(\theta_a - \tilde{\theta})}{\xi(i, j, \tilde{\theta})} d\tilde{\theta} \tag{A19}$$

and

$$h_z^{(II)}(r_i, z_j, \theta_k) = \frac{J}{4\pi\mu_0} \cos\left(\frac{\theta_1 - \theta_2}{2}\right) \log\left[r_i - r\cos(\theta - \theta_k) + \xi(i, j, \theta_k)\right] \tag{A20}$$

## A.2. Tile Permanent Magnets Uniformy and Radially Magnetized

Let us now consider the magnetic field created by tile permanent magnets whose polarization is both uniform and radial. For this purpose, let us consider the parameters defined in Fig. 22.

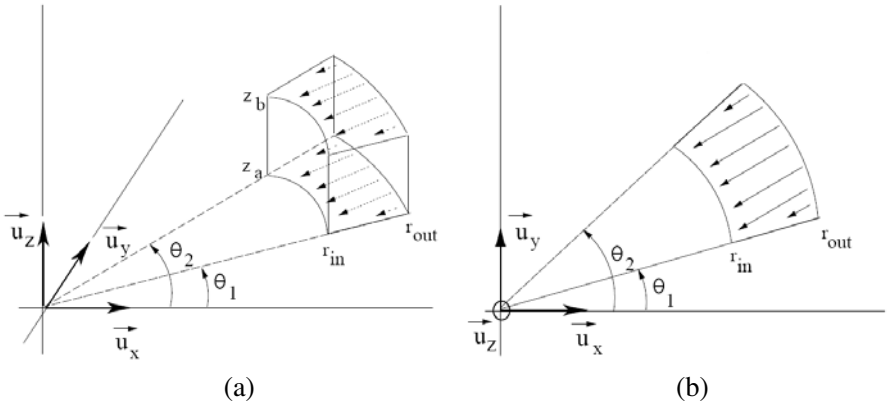


**Figure 22.** Representation of the configuration considered. The ring inner radius is $r_{\text{in}}$, the ring outer one is $r_{\text{out}}$, its height is $z_b - z_a$, its angular width is $\theta_2 - \theta_1$.

The radial component $H_r(r, \theta, z)$ of the magnetic field created by one tile permanent magnet uniformly magnetized can be expressed as

follows:

$$\begin{aligned}
& H_r(r,\theta,z) \\
= & +\frac{J}{4\pi\mu_0} r_{\text{in}}(-z+z_b)\mathbf{S}\left[r^2+r_{\text{in}}^2, 2rr_{\text{in}}, r^2+r_{\text{in}}^2+(z-z_b)^2, r_{\text{in}}\right] \\
& -\frac{J}{4\pi\mu_0} r_{\text{in}}(-z+z_a)\mathbf{S}\left[r^2+r_{\text{in}}^2, 2rr_{\text{in}}, r^2+r_{\text{in}}^2+(z-z_a)^2, r_{\text{in}}\right] \\
& +\frac{J}{4\pi\mu_0} r_{\text{out}}(-z+z_a)\mathbf{S}\left[r^2+r_{\text{out}}^2, 2rr_{\text{out}}, r^2+r_{\text{out}}^2+(z-z_a)^2, r_{\text{out}}\right] \\
& -\frac{J}{4\pi\mu_0} r_{\text{out}}(-z+z_b)\mathbf{S}\left[r^2+r_{\text{out}}^2, 2rr_{\text{out}}, r^2+r_{\text{out}}^2+(z-z_b)^2, r_{\text{out}}\right] \\
& +\frac{J}{4\pi\mu_0}\left(o(r_{\text{out}})-o(r_{\text{in}})\right) \\
& +\frac{J}{4\pi\mu_0}\left(p(r_{\text{out}})-p(r_{\text{in}})\right) \qquad \text{(A21)}
\end{aligned}$$

where

$$\begin{aligned}
o(r_1) = & -\xi((z_a-z)\left(\sin\left(\frac{\theta_2-\theta_1}{2}\right), r^2+r_1^2+(z-z_a)^2, r, r_1, \cos(\theta-\theta_2)\right) \\
& +\xi((z_b-z)\left(\sin\left(\frac{\theta_2-\theta_1}{2}\right), r^2+r_1^2+(z-z_b)^2, r, r_1, \cos(\theta-\theta_2)\right)
\end{aligned} \qquad \text{(A22)}$$

and

$$\begin{aligned}
p(r_1) = & -\xi((z_a-z)\left(\sin\left(\frac{\theta_2-\theta_1}{2}\right), r^2+r_1^2+(z-z_a)^2, r, r_1, \cos(\theta-\theta_1)\right) \\
& +\xi((z_b-z)\left(\sin\left(\frac{\theta_2-\theta_1}{2}\right), r^2+r_1^2+(z-z_b)^2, r, r_1, \cos(\theta-\theta_1)\right)
\end{aligned} \qquad \text{(A23)}$$

We define $\xi(y,u,r,r_1,s)$, $A$ and $B$ as follows:

$$\begin{aligned}
\xi(y,u,r,r_1,s) = & \frac{iy}{2\sqrt{s^2-1}\sqrt{r^2-u}}\left((1-s^2+s\sqrt{s^2-1})\log[A]\right) \\
& +\frac{iy}{2\sqrt{s^2-1}\sqrt{r^2-u}}\left(s^2-1+s\sqrt{s^2-1})\log[B]\right)
\end{aligned} \qquad \text{(A24)}$$

$$A = \frac{2i\left(rr_1(s^2-1)+r^2s(1-s+s\sqrt{s^2-1})\right)}{(1-s^2+s\sqrt{s^2-1})(r_1+r(\sqrt{s^2-1}-s))\sqrt{r^2-u}} + \frac{\sqrt{s^2-1}(-u+i\sqrt{r^2-u}\sqrt{r_1^2-2rr_1s+u})}{(1-s^2+s\sqrt{s^2-1})(r_1+r(\sqrt{s^2-1}-s))\sqrt{r^2-u}} \quad \text{(A25)}$$

and

$$B = \frac{2i\left(rr_1(s^2-1)-r^2s(-1+s^2+s\sqrt{s^2-1}\right)}{(s^2-1+s\sqrt{s^2-1})(r(s+\sqrt{s^2-1})-r_1)\sqrt{r^2-u}} + \frac{2\sqrt{s^2-1}(iu+\sqrt{r^2+u}\sqrt{r_1^2-2rr_1s+u})}{(s^2-1+s\sqrt{s^2-1})(r(s+\sqrt{s^2-1})-r_1)\sqrt{r^2-u}} \quad \text{(A26)}$$

The semi-analytical part $\mathbf{S}\left[i,j,k,l\right]$ is defined as follows:

$$\mathbf{S}\left[i,j,k,l\right] = \int_{\theta_1}^{\theta_2} \frac{\left(r-l\cos(\theta-\tilde{\theta})\right)\cos\left(\tilde{\theta}-\frac{\theta_1+\theta_2}{2}\right)}{\left(i-j\cos(\theta-\tilde{\theta})\right)\sqrt{k-j\cos(\theta-\tilde{\theta})}}d\tilde{\theta} \quad \text{(A27)}$$

The azimuthal component $H_\theta(r,\theta,z)$ of the magnetic field created by one tile permanent magnet uniformly magnetized can be expressed as follows:

$$\begin{aligned} & H_\theta(r,\theta,z) \\ = & +\frac{J}{4\pi\mu_0}r_{in^2}(-z+z_a)\mathbf{R}\left[r^2+r_{\text{in}}^2, 2rr_{\text{in}}, r^2+r_{\text{in}}^2+(z-z_a)^2\right] \\ & -\frac{J}{4\pi\mu_0}r_{in^2}(-z+z_b)\mathbf{R}\left[r^2+r_{\text{in}}^2, 2rr_{\text{in}}, r^2+r_{\text{in}}^2+(z-z_b)^2\right] \\ & -\frac{J}{4\pi\mu_0}r_{out^2}(-z+z_a)\mathbf{R}\left[r^2+r_{\text{out}}^2, 2rr_{\text{out}}, r^2+r_{\text{out}}^2+(z-z_a)^2\right] \\ & +\frac{J}{4\pi\mu_0}r_{out^2}(-z+z_b)\mathbf{R}\left[r^2+r_{\text{out}}^2, 2rr_{\text{out}}, r^2+r_{\text{out}}^2+(z-z_b)^2\right] \\ & +\frac{J}{4\pi\mu_0}\left(g(r_{\text{out}},h,\theta_2)-g(r_{\text{in}},h,\theta_2)-g(r_{\text{out}},0,\theta_2)+g(r_{\text{in}},0,\theta_2)\right) \\ & +\frac{J}{4\pi\mu_0}\left(w(r_{\text{out}},h,\theta_1)-w(r_{\text{in}},h,\theta_1)-g(r_{\text{out}},0,\theta_1)+g(r_{\text{in}},0,\theta_1)\right) \end{aligned} \quad \text{(A28)}$$

where

$$g(r_{\text{out}},h,\theta_i) = \sin\left(\frac{\theta_2-\theta_1}{2}\right)f(r_1,z,\theta_i) \quad \text{(A29)}$$

and

$$w(r_{\text{out}}, h, \theta_i) = \sin\left(\frac{\theta_2 - \theta_1}{2}\right) f(r_1, z, \theta_i) \tag{A30}$$

We define $f(r_1, z, \theta_i$ as follows:

$$\begin{aligned} & f(r_1, z, \theta_i) \\ = & -\frac{(-2a + b + r^2) \arctan\left[\frac{\sqrt{-4a+b+2(r^2+r_1^2)-r^2}(z-z_1)}{\sqrt{-4a+b+2(r^2+r_1^2)-r^2}\sqrt{-b+r^2}}\right]}{\sqrt{-4a + b + 2(r^2 + r_1^2) - r^2}\sqrt{-b + r^2}} \sin(\theta - \theta_i) \\ & - \log\left[z - z_1 + \sqrt{-2a + r^2 + r_1^2 + (z - z_1)^2}\right] \end{aligned} \tag{A31}$$

$$a = r r_1 \cos(\theta - \theta_i) \tag{A32}$$

$$b = r^2 \cos(2(\theta - \theta_i)) \tag{A33}$$

Here, the semi-analytical part is given by:

$$\mathbf{R}\,[i, j, k] = \int_{\theta_1}^{\theta_2} \frac{\cos(\tilde{\theta} - \frac{\theta_1 + \theta_2}{2}) \sin(\theta - \tilde{\theta})}{\left(i - j\cos(\theta - \tilde{\theta})\sqrt{k - j\cos(\theta - \tilde{\theta})}\right)} d\tilde{\theta} \tag{A34}$$

The axial component $H_z(r, \theta, z)$ of the magnetic field created by one tile permanent magnet uniformly magnetized can be expressed as follows:

$$\begin{aligned} & H_z(r, \theta, z) \\ = & \frac{J}{4\pi\mu_0} r_{\text{in}} \mathbf{T}\left[r^2 + r_{\text{in}}^2 + (z - z_b)^2, 2r r_{\text{in}}\right]) \\ & - \frac{J}{4\pi\mu_0} r_{\text{in}} \mathbf{T}\left[r^2 + r_{\text{in}}^2 + (z - z_a)^2, 2r r_{\text{in}}\right] \\ & + \frac{J}{4\pi\mu_0} r_{\text{out}} \mathbf{T}\left[r^2 + r_{\text{out}}^2 + (z - z_a)^2, 2r r_{\text{out}}\right] \\ & - \frac{J}{4\pi\mu_0} r_{\text{out}} \mathbf{T}\left[r^2 + r_{\text{out}}^2 + (z - z_b)^2, 2r r_{\text{out}}\right] \\ & + \frac{J}{4\pi\mu_0} (\eta(r_{\text{in}}, z_a) - \eta(r_{\text{in}}, z_b) - \eta(r_{\text{out}}, z_a) + \eta(r_{\text{out}}, z_b)) \\ & + \frac{J}{4\pi\mu_0} (\beta(r_{\text{in}}, z_a) - \beta(r_{\text{in}}, z_b) - \beta(r_{\text{out}}, z_a) + \beta(r_{\text{out}}, z_b)) \end{aligned} \tag{A35}$$

where

$$\eta(x, y) = \sin\left(\frac{\theta_2 - \theta_1}{2}\right) \log\left[x - r\cos(\theta - \theta_2) + t(\theta_2)\right] \tag{A36}$$

and

$$\beta(x,y) = \sin\left(\frac{\theta_2-\theta_1}{2}\right)\log\left[x - r\cos(\theta-\theta_1) + t(\theta_1)\right] \tag{A37}$$

with

$$t(\theta_i) = \sqrt{r^2 + x^2 + (z-y)^2 - 2rx\cos(\theta-\theta_i)} \tag{A38}$$

The semi-analytical part is given by:

$$\mathbf{T}\left[i,j\right] = \int_{\theta_1}^{\theta_2} \frac{\cos\left(\tilde{\theta} - \frac{\theta_1+\theta_2}{2}\right)}{\sqrt{i - j\cos(\theta-\tilde{\theta})}} d\tilde{\theta} \tag{A39}$$

## REFERENCES


1. Halbach, K., "Strong rare earth cobalt quadrupoles," *IEEE Trans. Magn.*, Vol. 26, No. 3, 3882–3884, 1979.
2. Halbach, K., "Design of permanent multiple magnets with oriented rec material," *Nucl. Inst. Meth.*, Vol. 169, 1–10, 1980.
3. Marinescu, M. and N. Marinescu, "Compensation of anisotropy effects in flux-confining permanent-magnet structures," *IEEE Trans. Magn.*, Vol. 25, No. 5, 3899–3901, 1989.
4. Marinescu, M. and N. Marinescu, "Anisotropy effects in permanent multiple magnets," *IEEE Trans. Magn.*, Vol. 20, No. 5, 3882–3884, 1984.
5. Marinescu, M. and N. Marinescu, "New concept of permanent-magnet excitation for electrical machines," *IEEE Trans. Magn.*, Vol. 28, 1390–1393, 1992.
6. Ravaud, R., G. Lemarquand, V. Lemarquand, and C. Depollier, "Analytical calculation of the magnetic field created by permanent-magnet rings," *IEEE Trans. Magn.*, Vol. 44, No. 8, 1982–1989, 2008.
7. Babic, S. and C. Akyel, "Improvement of the analytical calculation of the magnetic field produced by permanent magnet rings," *Progress In Electromagnetics Research C*, Vol. 5, 71–82, 2008.
8. Furlani, E. P., *Permanent Magnet and Electromechanical Devices: Materials, Analysis and Applications*, Academic Press, 2001.
9. Selvaggi, J. P., S. Salon, O. M. Kwon, and M. Chari, "Computation of the three-dimensional magnetic field from solid permanent-magnet bipolar cylinders by employing toroidal harmonics," *IEEE Trans. Magn.*, Vol. 43, No. 10, 3833–3839, 2007.

10. Azzerboni, B. and G. Saraceno, "Three-dimensional calculation of the magnetic field created by current-carrying massive disks," *IEEE Trans. Magn.*, Vol. 34, No. 5, 2601–2604, 1998.
11. Rakotoarison, H. L., J. P. Yonnet, and B. Delinchant, "Using coulombian approach for modeling scalar potential and magnetic field of a permanent magnet with radial polarization," *IEEE Trans. Magn.*, Vol. 43, No. 4, 1261–1264, 2007.
12. Durand, E., *Magnetostatique*, Masson Editeur, Paris, France, 1968.
13. Babic, S. and C. Akyel, "Magnetic force calculation between thin coaxial circular coils in air," *IEEE Trans. Magn.*, Vol. 44, No. 4, 445–452, 2008.
14. Babic, S., C. Akyel, S. Salon, and S. Kincic, "New expressions for calculating the magnetic field created by radial current in massive disks," *IEEE Trans. Magn.*, Vol. 38, No. 2, 497–500, 2002.
15. Babic, S., S. Salon, and C. Akyel, "The mutual inductance of two thin coaxial disk coils in air," *IEEE Trans. Magn.*, Vol. 40, No. 2, 822–825, 2004.
16. Furlani, E. P., S. Reznik, and A. Kroll, "A three-dimensonal field solution for radially polarized cylinders," *IEEE Trans. Magn.*, Vol. 31, No. 1, 844–851, 1995.
17. Furlani, E. P., "Field analysis and optimization of ndfeb axial field permanent magnet motors," *IEEE Trans. Magn.*, Vol. 33, No. 5, 3883–3885, 1997.
18. Furlani, E. P. and M. Knewston, "A three-dimensional field solution for permanent-magnet axial-field motors," *IEEE Trans. Magn.*, Vol. 33, No. 3, 2322–2325, 1997.
19. Furlani, E. P., "A two-dimensional analysis for the coupling of magnetic gears," *IEEE Trans. Magn.*, Vol. 33, No. 3, 2317–2321, 1997.
20. Mayergoyz, D. and E. P. Furlani, "The computation of magnetic fields of permanent magnet cylinders used in the electrophotographic process," *J. Appl. Phys.*, Vol. 73, No. 10, 5440–5442, 1993.
21. Azzerboni, B. and E. Cardelli, "Magnetic field evaluation for disk conductors," *IEEE Trans. Magn.*, Vol. 29, No. 6, 2419–2421, 1993.
22. Azzerboni, B., E. Cardelli, M. Raugi, A. Tellini, and G. Tina, "Magnetic field evaluation for thick annular conductors," *IEEE Trans. Magn.*, Vol. 29, No. 3, 2090–2094, 1993.
23. Yonnet, J. P., *Rare-earth Iron Permanent Magnets*, Ch. Magnetomechanical Devices, Oxford Science Publications, 1996.

24. Blache, C. and G. Lemarquand, "New structures for linear displacement sensor with hight magnetic field gradient," *IEEE Trans. Magn.*, Vol. 28, No. 5, 2196–2198, 1992.
25. Zhu, Z. and D. Howe, "Analytical prediction of the cogging torque in radial-field permanent magnet brushless motors," *IEEE Trans. Magn.*, Vol. 28, No. 2, 1371–1374, 1992.
26. Blache, C. and G. Lemarquand, "High magnetic field gradients in flux confining permanent magnet structures," *Journal of Magnetism and Magnetic Materials*, Vol. 104, 1111–1112, 1992.
27. Wang, J., G. W. Jewell, and D. Howe, "Design optimisation and comparison of permanent magnet machines topologies," *IEE. Proc. Elect. Power Appl.*, Vol. 148, 456–464, 2001.
28. Lemarquand, V., J. F. Charpentier, and G. Lemarquand, "Nonsinusoidal torque of permanent-magnet couplings," *IEEE Trans. Magn.*, Vol. 35, No. 5, 4200–4205, 1999.
29. Abele, M., J. Jensen, and H. Rusinek, "Generation of uniform high fields with magnetized wedges," *IEEE Trans. Magn.*, Vol. 33, No. 5, 3874–3876, 1997.
30. Lemarquand, G. and V. Lemarquand, "Annular magnet position sensor," *IEEE. Trans. Magn.*, Vol. 26, No. 5, 2041–2043, 1990.
31. Aydin, M., Z. Zhu, T. Lipo, and D. Howe, "Minimization of cogging torque in axial-flux permanent-magnet machines: design concepts," *IEEE Trans. Magn.*, Vol. 43, No. 9, 3614–3622, 2007.
32. Yong, L., J. B. Zou, and Y. P. Lu, "Optimum design of magnet shape in permanent-magnet synchronous motors," *IEEE Trans. Magn.*, Vol. 39, No. 11, 3523–4205, 2003.
33. Bancel, F. and G. Lemarquand, "Three-dimensional analytical optimization of permanent magnets alternated structure," *IEEE Trans. Magn.*, Vol. 34, No. 1, 242–247, 1998.
34. Elies, P. and G. Lemarquand, "Analytical study of radial stability of permanent magnet synchronous couplings," *IEEE Trans. Magn.*, Vol. 35, No. 4, 2133–2136, 1999.
35. Charpentier, J. F., V. Lemarquand, and G. Lemarquand, "A study of permanent-magnet couplings with progressive magnetization using analytical exact formulation," *IEEE Trans. Magn.*, Vol. 35, No. 5, 4206–4217, 1999.
36. Berkouk, M., V. Lemarquand, and G. Lemarquand, "Analytical calculation of ironless loudspeaker motors," *IEEE Trans. Magn.*, Vol. 37, No. 2, 1011–1014, 2001.
37. Lemarquand, G., "Ironless loudspeakers," *IEEE Trans. Magn.*, Vol. 43, No. 8, 3371–3374, 2007.

38. Ravaud, R., G. Lemarquand, V. Lemarquand, and C. Depollier, "The three exact components of the magnetic field created by a radially magnetized tile permanent magnet," *Progress In Electromagnetics Research*, PIER 88, 307–319, 2008.
39. Ravaud, R., G. Lemarquand, V. Lemarquand, and C. Depollier, "Discussion about the analytical calculation of the magnetic field created by permanent magnets," *Progress In Electromagnetics Research B*, Vol. 11, 281–297, 2009.
40. http://www.univ-lemans.fr/∼glemar.